Signature of Mott-Insulator Transition with Ultracold Fermions in a One-Dimensional Optical Lattice

Xia-Ji Liu,[1] Peter D. Drummond,[1] and Hui Hu[2,3]

[1]*ARC Centre of Excellence for Quantum-Atom Optics, Department of Physics, University of Queensland, Brisbane, Queensland 4072, Australia*

[2]*NEST-INFM and Classe di Scienze, Scuola Normale Superiore, I-56126 Pisa, Italy*

[3]*Interdisciplinary Center of Theoretical Studies, Chinese Academy of Science, P. O. Box 2735, Beijing 100084, People's Republic of China*

(Received 18 October 2004; published 8 April 2005)

Using the exact Bethe ansatz solution of the Hubbard model and Luttinger liquid theory, we investigate the density profiles and collective modes of one-dimensional ultracold fermions confined in an optical lattice with a harmonic trapping potential. We determine a generic phase diagram in terms of a characteristic filling factor and a dimensionless coupling constant. The collective oscillations of the atomic mass density, a technique that is commonly used in experiments, provide a signature of the quantum phase transition from the metallic phase to the Mott-insulator phase. A detailed experimental implementation is proposed.

DOI: 10.1103/PhysRevLett.94.136406 PACS numbers: 71.10.Pm, 03.75.Kk, 03.75.Ss, 71.30.+h

Introduction.—The Mott metal-insulator transition (MMIT) is a fundamental concept in strongly correlated many-body systems. Recent experiments with ultracold atomic gases in optical lattices are paving the way to explore such quantum phase transitions in a well-controlled manner. The MMIT with bosonic atoms has been demonstrated by Greiner *et al.* [1]. A demonstration with fermions has not yet been realized experimentally, although its realization is within reach of present-day techniques. In the fermionic case, the relevant theory is the widely studied Hubbard model. This is the simplest lattice model of interacting fermions, and is exactly soluble in one dimension.

A gas of single component ^{40}K atoms in a parallel plane lattice has already been created by the LENS group, thanks to rapid progress in the cooling of fermions to temperatures below a micro-Kelvin. This demonstrated a noninteracting band insulator behavior [2–4] through the observation of dipole mode oscillations. An interacting gas of ultracold fermions with two populated hyperfine levels in a one-dimensional lattice is also feasible, thus offering the possibility of observing the fermionic MMIT.

Motivated by this opportunity, we address the problem of how to detect the emergence of fermionic Mott-insulator phases in real experiments with ultracold fermions. With optical lattices, a harmonic potential is necessary to prevent the atoms from escaping, so that the Mott-insulator phase is restricted to an insulator domain at the center of the trap, and coexists with two compressible metallic wings. Therefore, the insulator phase cannot be characterized by a global compressibility as in the unconfined case. Rigol *et al.* [5] showed that a properly defined local compressibility exhibits critical behavior on approaching the metal-insulator boundary.

In this Letter we show that collective oscillations of the atomic mass density, an indicator of compressibility, can be utilized to monitor the emergence of the Mott-insulator phase. We consider a zero temperature, one-dimensional Hubbard model with a harmonic potential, as a model of an ultracold two-component fermionic atomic cloud in a deep optical lattice with strong radial and weak axial confinement. Based on the exact Bethe ansatz solution of the homogeneous 1D Hubbard model [6], together with the local density approximation (LDA), we calculate the density profile of the cloud as functions of a characteristic filling factor and coupling constant. This leads to a generic phase diagram including a metallic phase and a Mott-insulator phase. We then investigate the low-energy collective density oscillations of the cloud in different phases using Luttinger liquid (LL) theory [7], which describes long-wavelength hydrodynamic behavior.

We find that in the metallic phase the collective oscillation is an overall motion that goes through all sites of the cloud. This quenches gradually towards the phase transition point, with the mode frequency decreasing monotonically to zero. After entering the Mott-insulator phase, the density oscillation revives, but is restricted to the compressible wings. Therefore, a sharp dip appears in all collective mode frequencies in the vicinity of the phase boundary, giving a clear signature of the MMIT.

Phase diagram.—We consider the 1D Hubbard model [6], as a prototype for N ($N/2 = N_\uparrow = N_\downarrow$) interacting fermions in deep optical lattices, with a Hamiltonian given by

$$\mathcal{H}_0/t_h = u\sum_i n_{i\uparrow}n_{i\downarrow} - \sum_{i\sigma}(c^+_{i\sigma}c_{i+1\sigma} + \text{H.c.}). \quad (1)$$

Here t_h and u ($u > 0$) are the hopping parameter and the dimensionless on-site repulsion, respectively. The spin $\sigma = \uparrow, \downarrow$ represents different hyperfine states. The axial harmonic trap adds a site dependent potential to the Hamiltonian so that

$$\mathcal{H} = \mathcal{H}_0 + \sum_{i\sigma} \frac{m\omega_0^2}{2} d^2 i^2 n_{i\sigma}, \tag{2}$$

where ω_0 is the bare trapping frequency and $d = \lambda/2$ is the lattice periodicity, while λ is the wavelength of standing waves used to create the 1D optical lattice. We describe the inhomogeneous gas, Eq. (2), within the LDA. This amounts to determining the chemical potential of the gas from the local equilibrium condition,

$$\mu = \mu_{\rm hom}[n(x), u] + \frac{m\omega_0^2}{2} d^2 x^2. \tag{3}$$

We also impose a normalization condition, $\sum_{i=-\infty}^{+\infty} n(i) = \int_{-\infty}^{+\infty} n(x)dx = N$, using $\mu_{\rm hom}[n(x), u]$ as the chemical potential of a homogeneous system with a local filling factor $n(x)$ $[0 \le n(x) \le 2]$ [8]. In the framework of LDA, we replaced the site index i with a dimensionless variable x. The LDA is applicable in the limit of a large lattice with a slowly varying trapping potential. In other words, the use of LDA is justified if the size of the gas is much larger than the harmonic oscillator length $\sqrt{\hbar/m\omega_0}$, implying $\mu \gg \omega_0$ or $N \gg 1$. Because of the optical lattice, the single-particle trapping frequency is renormalized to $\omega_{\rm eff} = (m/m^*)^{1/2}\omega_0$, with an effective mass $m^* = \hbar^2/(2d^2 t_h)$. We also define a dimensionless frequency, $\omega = \hbar\omega_{\rm eff}/(2t_h)$, with corresponding dimensionless time $\tau = t\omega_{\rm eff}/\omega$.

To construct the phase diagram, it is useful to introduce two parameters: $\kappa = u^2/(16N\omega)$ is the interaction strength, and $\nu = 2\sqrt{N\omega}/\pi$ is the characteristic filling factor. We clarify the physical meanings of these parameters by considering two limiting cases.

(i) In the limit of a dilute Fermi cloud $[n(i) \to 0]$, the Hubbard model reduces to Yang's exactly solvable Fermi gas model. Therefore, the homogeneous chemical potential takes the form $\mu_{\rm hom}[n, u] = (2t_h)(\pi^2 n^2/8)\mu'_{\rm hom}[u/(2n)]$ up to an irrelevant constant. The function $\mu'_{\rm hom}$ is obtained by solving a set of integral equations [9].

In terms of the dimensionless chemical potential $\tilde{\mu} = 8\mu/(u^2 t_h)$ and the rescaled coordinate $\tilde{x} = 4\omega x/u$, the local equilibrium and normalization conditions can be reexpressed as $\pi^2/[2\gamma^2(\tilde{x})]\mu'_{\rm hom}[\gamma(\tilde{x})] + \tilde{x}^2/2 = \tilde{\mu}$ and $\int_{-\infty}^{+\infty} 2/\gamma(\tilde{x})d\tilde{x} = 16N\omega/u^2$, where $\gamma(\tilde{x}) = u/[2n(\tilde{x})]$. These equations indicate that the coupling strength is $\kappa = u^2/(16N\omega)$, where $\kappa \ll 1$ corresponds to weak couplings and $\kappa \gg 1$ is the strongly interacting regime.

(ii) In the noninteracting limit, $\mu_{\rm hom}[n, u = 0] = -2t_h \times \cos(\pi n/2) \overset{n\to 0}{\approx} 2t_h(-1 + \pi^2 n^2/8)$. It is straightforward to show that the central number density is $n(x = 0) = 2\sqrt{N\omega}/\pi$, which we define as the characteristic filling factor ν.

We determine the phase diagram in Fig. 1(a) from the density profiles. Five phases (or mixed phases) are identified by plotting the central density $n(x = 0)$ as a function of ν for different values of κ, as shown in Figs. 1(b)–1(d) and explained in the figure caption. In addition, various

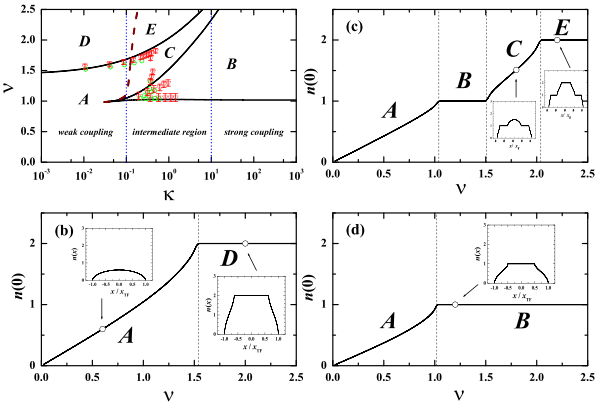

FIG. 1 (color online). Phase diagram of one-dimensional confined Fermi gases in optical lattices. *A*: a pure metallic phase. *B*: a single Mott-insulator domain at the center, accompanied by two metallic wings. *C*: a metallic phase at the center surrounded with Mott-insulator plateaus. *D*: a band insulator at the center with metallic wings outside. *E*: a band insulator at the trap center surrounded by metallic regions, in turn surrounded by Mott insulators. We have plotted a dashed line to illustrate the crossover behavior from *A* to *C*, or *D* to *E*. The empty symbols are the results from quantum Monte Carlo simulations [5]. In (b), (c) and (d), the central densities $n(x = 0)$ as a function of ν have been plotted for three values of $\kappa = 0.01$, 1, and 100. The dashed lines in these figures divide the system into different phases and the corresponding typical density profiles are shown in insets.

interaction regimes are illustrated explicitly by two dotted lines in Fig. 1(a), where $\kappa < 0.1$ corresponds to weak couplings, $\kappa > 10$ to strong couplings, and an intermediate regime is in between. In the weak coupling limit ($\kappa = 0.01$), the cloud is noninteracting. An increase of the characteristic filling factor changes it from a metal to a band insulator. In the strong coupling regime ($\kappa = 100$), the cloud behaves like a noninteracting *spinless* Tonks gas. It becomes a Mott insulator with increasing ν, which can also be understood as a band insulator in a spinless gas. In the intermediate coupling regime, the existence of the trap leads to a coexistence of metallic and insulating phases, labeled *C* and *E*, that have no correspondence in the unconfined case. An example is shown in Fig. 1(c) to illustrate the successive emergence of mixed phases *C* and *E* as ν increases.

A similar phase diagram of ultracold fermions in 1D optical lattices has been proposed previously in Ref. [5] using quantum Monte Carlo calculations. Our results for the phase boundaries are in quantitative agreement with their findings in the same parameter space that has been simulated. This is expected since the LDA should work well for these parameters. Since our theory uses an exact analytic solution, together with the asymptotically exact LDA, this verifies the previous numerical work. The discrepancy in determining the crossover boundary from *A* to *C* or *D* to *E* is due to the use of different criteria.

The phase diagram in Ref. [5] covers only the weak coupling and intermediate regimes of $\kappa \lesssim 1.0$. We have

extended their phase diagram to the strongly interacting regime. This extension turns out to be crucial from the experimental point of view. As we shall see in Figs. 2(a) and 2(c), the collective modes behave distinctly in different interaction regimes. Let us now consider in detail these collective density oscillations, which are of primary interest in the present Letter.

Collective density oscillations.—We describe the low-energy dynamics of density fluctuations of metallic regions in each phase using the LL model of the 1D Fermi gas in optical lattices [7], where the Hamiltonian can be written as

$$\mathcal{H}_{\mathrm{LL}} = \sum_{\nu=\rho,\sigma} \int dx \frac{u_\nu(x)}{2}\left[K_\nu(x)\Pi_\nu^2 + \frac{1}{K_\nu(x)}\left(\frac{\partial\phi_\nu}{\partial x}\right)^2\right]. \tag{4}$$

Here u_ρ and u_σ are the density and spin velocities, respectively, and K_ρ and K_σ are the Luttinger exponents of long-wavelength correlation functions. These parameters in a spatially homogeneous gas can be calculated from the Bethe ansatz solution of the 1D Hubbard model [8,10]. In the Hamiltonian, we have already used the LDA, i.e., $u_\nu(x) \equiv u_\nu(n(x))$ and $K_\nu(x) \equiv K_\nu(n(x))$. The canonical momenta Π_ν are conjugate to the phases ϕ_ν, i.e., $[\phi_\nu(x), \Pi_\mu(x')] = i\delta_{\mu\nu}\delta(x-x')$. Physically, the gradients of the phases $\partial_x\phi_\nu(x)$ are proportional to the density (or spin density) fluctuations, $\delta n_\nu(x) = -\partial_x\phi_\nu(x)$, while the momenta $\Pi_\nu(x)$ are proportional to the density (or spin density) currents, $j_\nu(x) = u_\nu(x)K_\nu(x)\Pi_\nu(x)$.

From this linearized Hamiltonian, we derive the hydrodynamic equation of motion

$$\frac{\partial^2\delta n_\nu}{\partial\tau^2} = \frac{\partial}{\partial x}\left[u_\nu(x)K_\nu(x)\frac{\partial}{\partial x}\left(\frac{u_\nu(x)}{K_\nu(x)}\delta n_\nu\right)\right]. \tag{5}$$

Hereafter we focus on the readily observable density modes. We consider the nth eigenmode with $\delta n_\rho(x) \sim \delta n_\rho(x)\exp(i\omega_n\tau)$ and substitute it into Eq. (5). The resulting equation for $\delta n_\rho(x)$ is solved using boundary conditions which require the current $j_\rho(x)$ to vanish [11]. The details, together with the interesting question of spin-charge separation, will be presented elsewhere [12].

Figure 2 shows the square of frequencies of the breathing mode and of the dipole mode at fixed values of ν and of κ. For a constant value of κ, the remarkable feature shown in Figs. 2(b) and 2(d) is the appearance of a sharp dip at a particular value of the characteristic filling factor, which has been identified as the transition point from a metal to an insulator. On the left side of the transition point, the cloud is a pure metal and the density fluctuates at all sites. The decrease of the frequency with increasing ν can be understood from the fact that in the homogeneous case the cloud has a soundlike spectrum, and the sound velocity u_ρ decreases as $u_\rho \propto 1-n$ on approaching the transition point at $n=1$, due to the opening of the charge gap. For larger filling, an insulating domain forms at the center of the trap,

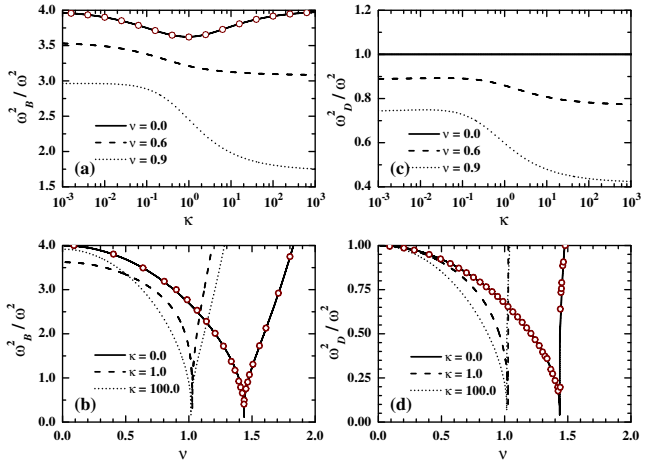

FIG. 2 (color online). Square of frequencies of the breathing mode (a), (b) and of the dipole mode (c), (d) at fixed values of ν and of κ. The circles in (a) are the predictions of the sum-rule approach, while the circles in (b) and (d) are the results for the noninteracting Fermi gas, obtained by solving the semiclassical Boltzmann kinetic equations.

in which the LL description breaks down. In response to a trap displacement, the center of mass will develop a quasi-static displacement in this case. Our theory is able to describe the *local* oscillations of the metallic wings around this new origin.

We have verified this expectation by using the semiclassical Boltzmann kinetic theory for a noninteracting cloud [4,13]. As ν increases, the metallic wings shrink in size and become less compressible. Therefore the mode frequency rises after crossing the transition point. This is the central result of this Letter. The Boltzmann theory also lets us investigate nonlinear damping effects, which we find increase rapidly with trap displacement [13]. These are absent in the LL theory, which only treats small displacements.

The application of the LL theory for low-energy dynamics of the 1D Hubbard model in the unconfined case is already well accepted in condensed matter physics [10]. In the presence of a trap, we would expect that the LDA is still applicable for describing the dynamics of the cloud. To this aim, we have examined the validity of the LL theory within LDA for collective oscillations by using alternative methods in two limiting cases. (i) In Fig. 2(a) the open circles are the prediction of m_3/m_1 or m_1/m_{-1} sum rules at $\nu \to 0$ [12,14]. The excellent agreement shows that the LL theory is correct at low density for *arbitrary coupling strengths*. (ii) On the other hand, for a noninteracting gas at a *finite* filling factor, we calculate the mode frequency by solving the semiclassical Boltzmann kinetic equation [13]. As shown by open circles in Figs. 2(b) and 2(d), this leads again to the same result obtained by the LL theory. Combining these two observations, we expect that the LL theory within the LDA is valid for finite filling factor at arbitrary couplings, under the required conditions.

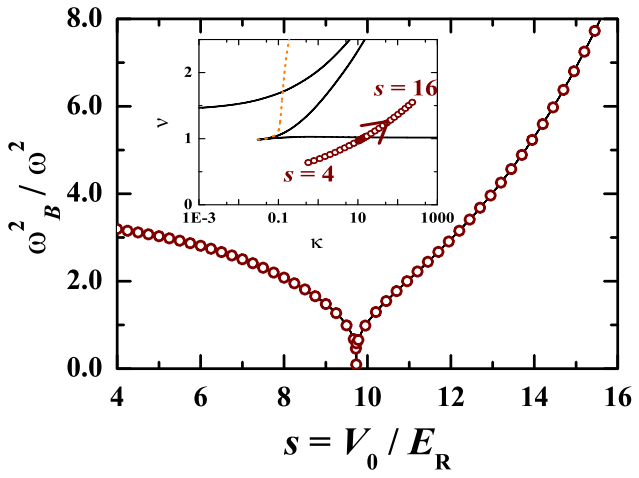

FIG. 3 (color online). A proposed experimental scheme. The square of breathing mode frequency has been plotted as a function of the depth of the lattice potential s for a gas of potassium atoms. The inset shows the path in the phase diagram with increasing s.

Experimental proposal.—In recent experiments, an array of quantum gases of bosonic ^{87}Rb atoms in 1D optical lattices has been created [15]. The gas is first subjected to a combined potential of a harmonic trap and deep transverse standing waves. An additional optical lattice with adjustable depth is then switched on in the axial direction to form the final configuration. An interacting Fermi gas of ^{40}K atoms in 3D lattices has also been demonstrated [16]. We expect that an array of interacting gases of ^{40}K atoms will be realized soon. Using the realistic parameters in Ref. [15] (with ^{87}Rb being replaced by ^{40}K), we have calculated t_h, $u = U/t_h$, and ω in a Gaussian approximation [17]. We have taken an interspecies s-wave scattering length $a_{3D} = +26a_B$ for ^{40}K atoms, where $a_B = 0.529$ Å is the Bohr radius. The value of a_{3D} is tunable by a Feshbach resonance. The typical number of atoms in each tube is $N = 15$, which is about the minimum required for the validity of LDA.

We show the square of frequencies of the breathing mode as a function of the depth s of the lattice potential in Fig. 3. Finite temperatures and/or nonlinear effects due to finite amplitude oscillations, will lead to the decay of collective modes, and simultaneously weaken the sharpness of the frequency dip. In addition, the experiments currently average over many tubes of 1D interacting gases, where the number of atoms has a parabolic distribution. This will further reduce the dip signal. Nevertheless, the qualitative picture of the appearance of dip structure in the vicinity of MMIT transition should persist, and will be a signature of the entrance into the Mott-insulator phase.

Conclusions.—In summary, we present a phase diagram for 1D confined fermions in an optical lattice. We show that the behavior of the frequencies of collective density modes is distinct in each phase. Therefore, the phase diagram can be detected unambiguously by measuring density oscillations. This provides a useful tool for locating the quantum phase transition from the metallic phase to the Mott-insulator phase. We expect that a similar sensitivity of the mode frequencies with respect to the phase will arise in higher dimensions. Furthermore, this signature could be applied as well to a gas of 1D bosons in an optical lattice, since the behavior of its low-energy excitations in the superfluid phase falls in the same universality class as the LL theory.

Our investigation is based on the exact Bethe ansatz solution and the LL theory of 1D Hubbard model, with the effect of harmonic traps being incorporated in the LDA. We justified the use of LDA in several limiting cases, both for static and dynamical properties. To further examine the validity of LDA for dynamics, more complicated numerical simulations are necessary. Possible candidates are fermionic phase-space [18] or time-dependent density-matrix renormalization group method [19]. This is beyond the scope of the present Letter.

We are indebted to M. Rigol and F. Werner for useful discussions. X.-J. L. and P. D. D. gratefully acknowledge support by the Australian Research Council. H. H. was partially supported by INFM under the PRA-Photonmatter Programme.

[1] M. Greiner *et al.*, Nature (London) **415**, 39 (2002).
[2] L. Pezze *et al.*, Phys. Rev. Lett. **93**, 120401 (2004).
[3] C. Hooley and J. Quintanilla, Phys. Rev. Lett. **93**, 080404 (2004).
[4] T. A. B. Kennedy, Phys. Rev. A **70**, 023603 (2004).
[5] M. Rigol *et al.*, Phys. Rev. Lett. **91**, 130403 (2003).
[6] E. H. Lieb and F. Y. Wu, Phys. Rev. Lett. **20**, 1445 (1968).
[7] A. Recati *et al.*, Phys. Rev. Lett. **90**, 020401 (2003).
[8] C. F. Coll, Phys. Rev. B **9**, 2150 (1974).
[9] C. N. Yang, Phys. Rev. Lett. **19**, 1312 (1967).
[10] H. J. Schulz, Phys. Rev. Lett. **64**, 2831 (1990).
[11] R. Combescot and X. Leyronas, Phys. Rev. Lett. **89**, 190405 (2002).
[12] X.-J. Liu, P. D. Drummond, and H. Hu (unpublished).
[13] X.-J. Liu and P. D. Drummond (unpublished).
[14] These sum rules are derived by using the formulas in E. Lipparini and S. Stringari, Phys. Rep. **175**, 103 (1989).
[15] B. Paredes *et al.*, Nature (London) **429**, 277 (2004).
[16] M. Köhl *et al.*, Phys. Rev. Lett. **94**, 080403 (2005).
[17] The Gaussian approximation for the hopping parameter t_h becomes less accurate for a deep lattice depth. A better estimation of t_h can be found in W. Zwerger, J. Opt. B, **5**, S9 (2003).
[18] J. F. Corney and P. D. Drummond, Phys. Rev. Lett. **93**, 260401 (2004).
[19] C. Kollath *et al.*, cond-mat/0411403.